Integrated Magnetic for LLC Resonant Converter

Bo Yang, Rengang Chen and Fred C. Lee

Center for Power Electronics Systems
The Bradley Department of Electrical and Computer Engineering
Virginia Polytechnic Institute and State University
Blacksburg, VA 24061 USA
Email: boyang@vpec.vt.edu

Abstract- **A new LLC resonant converter is proposed for Front End DC/DC conversion in Distributed Power System recently. This converter shows some potential benefits in this application. This paper proposes several integrated magnetic design for LLC Resonant Converter. For this converter, it has three magnetic components. With magnetic integration, firstly number of components can be reduced; secondly, flux ripple cancellation is achieved so that core loss is reduced. From these benefits, higher power density can be achieved. In design of the integrated magnetic structure for LLC resonant converter, a general model of four winding integrated magnetic structure is derived which can be used to derive integrated magnetic structure for different topologies. Finally, test result is shown.**

I. Introduction

The increasing efforts on pushing to high power density and high efficiency DC/DC converter have lead us to develop converters capable of operating at higher switching frequency with high efficiency.

A novel LLC resonant converter is proposed for this application. Fig. 1 shows circuit diagram of LLC resonant converter. Compare with PWM converter, this topology provides lower switching loss and conduction loss so that it can achieve high efficiency and the potential of high frequency operation. Another advantage of this converter is that it can be optimized at high input voltage, which is not possible for known PWM converter.

Even with advanced topologies, to achieve high power density, magnetic design is still the key issue. With the increasing of switching frequency, magnetic loss and winding loss is surfacing as a main part of the total loss. There are many ways to reduce the magnetic loss and size. Integrated magnetic as one approach is been discussed intensively recently for a lot of applications [2][3][4][5].

With integrated magnetic technique, several magnetic components can be constructed in one magnetic core by sharing the magnetic path. Through magnetic integration, total number of components can be reduced. With sharing the magnetic path, flux ripple can be reduced. Hence, with magnetic integration, high efficiency and high power density magnetic can be constructed. As shown in [4] for front end DC/DC converter, all the magnetic components of a current doubler are integrated into one magnetic core.

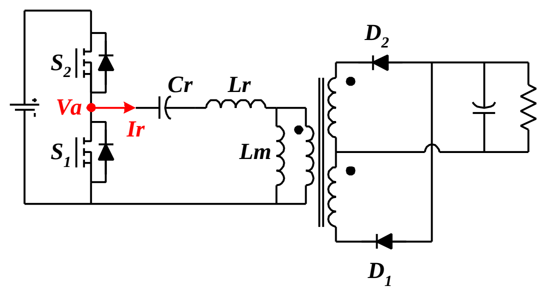

Fig. 1 LLC resonant converter

In this paper, first a design example of LLC resonant converter is given. Then the issues for integrated magnetic design are investigated. In order to do this, a general model for a widely used integrated magnetic structure is developed, which can be used to investigate different winding and gapping structures. Base on the general model, several integrated magnetic designs for LLC resonant converter are investigated and compared. The pros and cons of each design are analyzed. Finally, a prototype is build and tested.

II. Design Example for LLC Resonant Converter

In this paper, a Front End DC/DC converter with LLC resonant topology will be used as an example. The specifications of this converter are:

Input voltage range Vin:	300 to 400V,
Output voltage Vout:	48V
Output power range Po:	1.2kW.

The detail design procedure will not be discussed in the paper, only the design results are shown as following.

Transformer turn ratio:	4:1:1,
Resonant inductor:	14uH
Resonant capacitor:	0.047u,
Magnetizing inductance:	60uH.
Switching frequency range:	150kHz to 200kHz

The magnetic components structure is shown in Fig. 2. From Fig. 2 it can be found that this structure is the same as that of the real transformer. Leakage inductance can be used as Lr. Magnetizing inductance can be used as Lm. The problems with this implementation are: first, leakage inductance control is difficult. For the LLC resonant converter, Lr value is critical since it will determine the operating point. Second, when the resonant inductor Lr is built like this, the leakage inductance will not only exist on the primary side, it will also exist on the secondary side of the transformer. So the result get from real transformer will be as in Fig.3. L_{lp} and L_{ls} have similar values when reflected to the same side of the transformer.

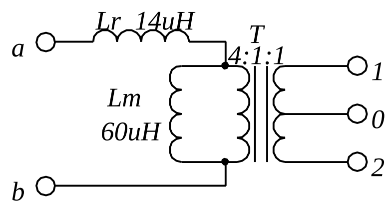

Fig. 2 Magnetic components for Front End DC/DC LLC resonant converter

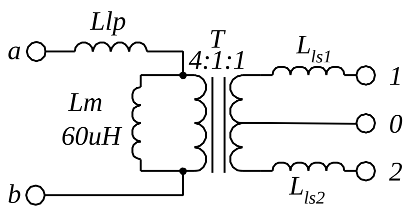

Fig. 3 Magnetic structures from Simple Transformer

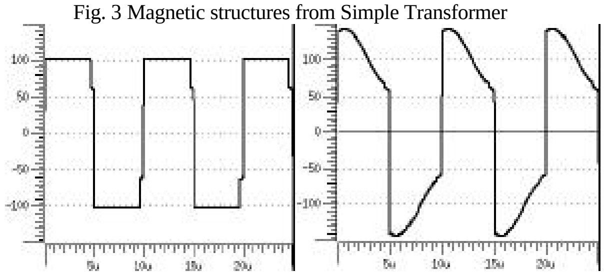

(a) (b)

Fig. 4 Simulation waveform of output diodes D1 D2 voltage stress

(a): with magnetic structure in Fig 2

(b) with magnetic structure in Fig3

When the leakage inductance exists on the secondary side, it will increase the voltage stress on secondary rectifier diode. So higher voltage-rating diodes are needed, which will increase the conduction loss. Fig 4 shows the simulate waveforms of secondary diodes with magnetic structure in Fig.2 and Fig.3. It can be seen that with inductor on the secondary side, the voltage stress of the diodes is much higher. The magnetic structure with precise control of Lr, Lm, while all resonant inductor are kept on the primary side, is needed.

III. Integrated Magnetic for LLC Resonant Converter

A. *Discrete Magnetic Solution for LLC Resonant Converter*

To discuss the magnetic integration, it is necessary to have a discrete design as the reference. In this part, a discrete design is presented and simulation result is shown to compare with integrated solution. For LLC resonant converter, the resonant inductor Lr has pure AC current through it, so soft ferrite core can be used for both inductor and transformer.

Fig. 5 shows the discrete design of the magnetic for LLC resonant converter. Two U cores were used to build the resonant inductor and gapped transformer. Fig.6 shows the simulation results of flux density in the core. For each U core, the cross-section area is $116.5mm^2$. Design results are as following: nl=12, np:ns:ns = 16:4:4, gap1=1.45mm and gap2=0.5mm.

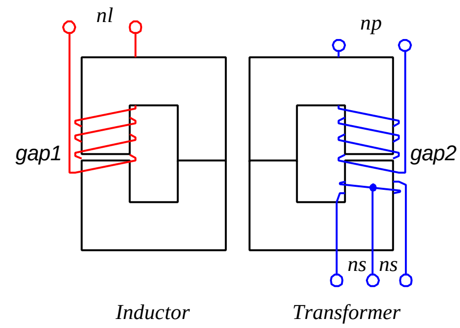

Fig. 5 Discrete magnetic design of LLC resonant converter

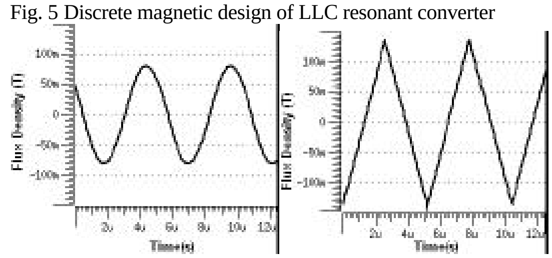

(a) Inductor (b) Transformer

Fig. 6 Flux density simulation result

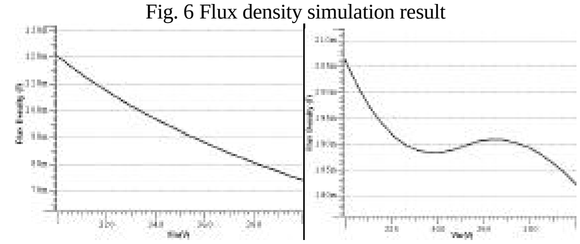

(a) Inductor (b) Transformer

Fig. 7 Flux density change with input voltage range

B. *Extraction of Common Structure for Integrated Magnetic*

In the past, a lot of research was done in integrated magnetic design for power converters. Reviewing those papers, it can be found that most of them are based on EE core structure. The difference between different designs is the placement of windings and air gaps.

In this part of the paper, the general circuit model of an EE core with four windings is used as a general structure as shown in Fig. 8. There are air gaps on each leg. This is a very commonly used structure, many integrated magnetic design for PWM converter also used this structure with some change on the air gap or winding placement [3][4].

The reason of choosing this structure for LLC resonant converter is as following:

To integrate two magnetic components, usually three magnetic paths are needed. In the LLC resonant converter, although there are three magnetic components, Lm and transformer T can be build within an air-gapped transformer. Therefore only two magnetic components: series resonant inductor Lr and gapped transformer T are needed to be integrated. An EE core structure will be a reasonable choice.

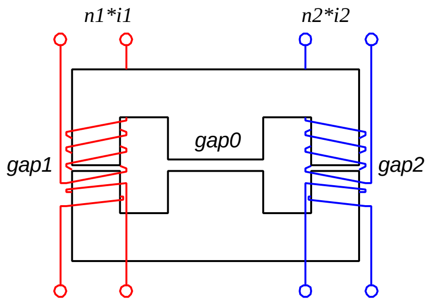

Fig. 8 general magnetic structures for Integrated magnetic

The proposed model is derived based on duality modeling theory [1]. Using this theory, the electrical circuit model of a physical magnetic structure can be obtained. All the component parameters in the model are related to the parameters of the physical magnetic structure. Fig 9 shows the reluctance model of magnetic structure shown in Fig. 8. Fig. 10 shows its equivalent electrical circuit model. In the structure, there exist two sets of ideal transformer and three inductors.

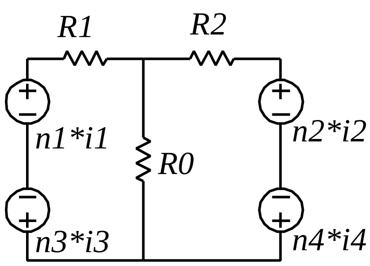

$$R1 = \frac{l_{gap1}}{m \cdot Ac} \qquad R2 = \frac{l_{gap2}}{m \cdot Ac} \qquad R0 = \frac{l_{gap0}}{m \cdot Ac}$$

Fig. 9 Reluctance model of general integrated magnetic structure

The turns ratio of the two ideal transformer are same, as in the real physical structure. The three inductors correspond to the three air gaps and they are all reflected to first winding n1. They can also be reflected to other windings as necessary. The values of each inductor are given in Fig. 13.

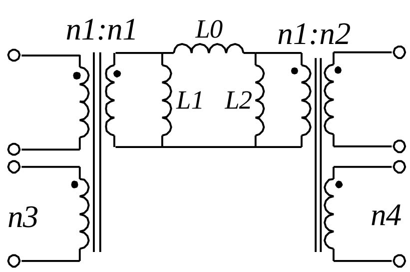

$$L1 = \frac{n_1^2}{R1} \qquad L2 = \frac{n_1^2}{R2} \qquad L0 = \frac{n_1^2}{R0}$$

Fig. 10 Circuit model of general integrated magnetic structure

Base on this circuit model, more integrated magnetic structures will be investigated.

*C. Integrated magnetic design **A** for LLC resonant converter*

From discrete design, just combine them together with an EE core, the two magnetic components can be integrated into one, as shown in Fig. 11.

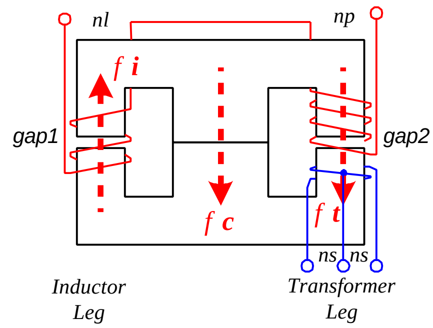

Fig. 11 Integrated Magnetic Designs A

E42/21/20 core is used. The cross-section area of is 233mm^2. For the outer legs, the cross-section area is the same as discrete design. Turn number nl, np and ns is the same as in discrete design. For this design, the inductor and transformer design is decoupled. Discrete design procedure still can be used. Fig. 9 shows the simulation result of for this structure.

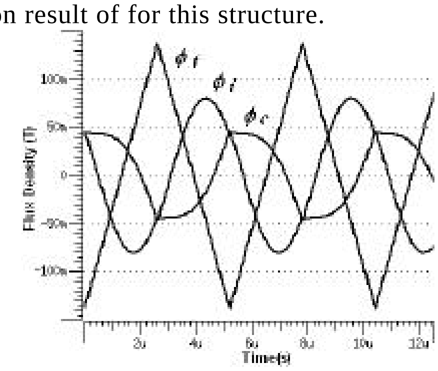

Fig. 12 Flux density simulation result for Design A

It can be seen from the simulation result that for inductor and transformer leg, the flux density is the same as discrete design. But for center leg, the flux density is much smaller than the discrete case. This will greatly reduce the magnetic loss in the big part of the magnetic component.

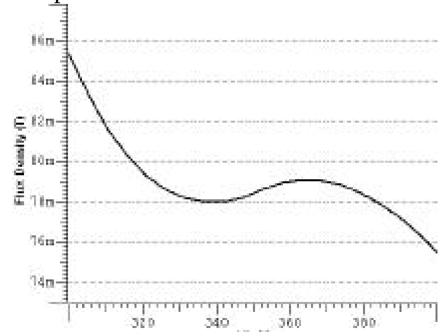

Fig. 13 Center leg flux density for different input voltage

Fig. 10 shows the center leg flux density for whole input voltage range. Compare with the discrete design, the flux density is only half of the transformer leg and much smaller than inductor leg within all input voltage range.

The shortcoming of this structure is the gapping. In this structure, two E cores are used. The air gap is on the two outer legs while there is no air gap on the center leg. This structure is not good in several senses: first, this core structure is standard. The standard core normally has air gap on the center leg or no air gap at all. Second, it is not a mechanical stable structure.

A desired core structure will have air gap on center leg or same air gap for all three legs.

D. Integrated magnetic design B for LLC resonant converter

As discussed previously, the air gapping in structure A is difficult to implement. In this part, the structure with same air gap for all three legs will be discussed. The winding structure is shown in Fig. 14.

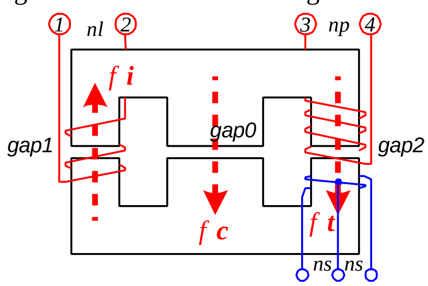

Fig. 14 Integrated Magnetic Designs A

The electrical model of this structure can be obtained from the proposed general structure. Compare this structure with the general structure; design B has only one winding on the left leg. By simplifying the general model, the following circuit model can be obtained, as shown in Fig. 15.

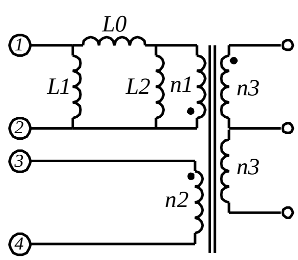

Fig. 15 Electrical circuit model of integrated magnetic structure B

Base on the electrical structure, there are two possible connections of the primary windings. Fig.16 shows one connection method, which connects the dot-marked terminal with unmarked terminal.

There are two operation modes for this circuit as shown in Fig. 17. One mode is n3 is connected to output. The other mode is both secondary windings are not connected. The equivalent circuit for these two modes will be derived separately.

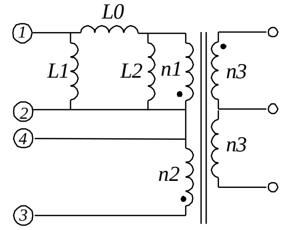

Fig. 16 Electrical model of connecting dot-marked terminal with unmarked terminal

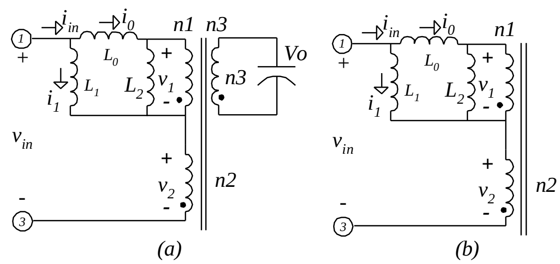

Fig.17 Two operation modes for LLC resonant converter

For operation mode (a), the following equations can be derived:

$$L1\frac{di_1}{dt}+\frac{n2}{n1}v_1=v_{in} \tag{1}$$

$$L0\frac{di_0}{dt}+v_1+\frac{n2}{n1}v_1=v_{in} \tag{2}$$

$$v_1=\frac{n1}{n3}Vo \tag{3}$$

$$i_0+i_1=i_{in} \tag{4}$$

From (1) to (4), the relationship of the input voltage, input current and output voltage can be expressed as following:

$$vin=\frac{L1\cdot L0}{L1+L0}\frac{di_{in}}{dt}+Vo\frac{1}{n3}(n2+n1\frac{L1}{L1+L0}) \tag{5}$$

From (5), the equivalent circuit during this mode can be obtained, as shown in Fig.18.

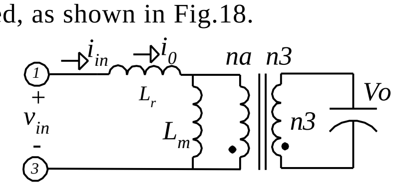

Fig.18 Equivalent-circuit for mode (a)

In this circuit, Lr, Lm and Na are given by the following equations:

$$Lr=\frac{L1\cdot L0}{L1+L0} \tag{6}$$

$$na=n2+n1\frac{L1}{L1+L0} \tag{7}$$

Operation mode (b) need to be analyzed to find out Lm. Following the same procedure as analyzing mode (a), another set of equations of mode (b) can be obtained, which will not be listed here. From mode (b) equations, the expression of Lm can be obtained, as shown in (8)

$$Lm = L2 \cdot \frac{na^2}{n1^2} \cdot \frac{L1 + L0}{L1 + L2 + L0} \qquad (8)$$

For the connection method shown in Fig. 19, the expressions of Lr, na and Lm can be obtain by following the same derivations as above. Those values are given by (9)-(11), respectively.

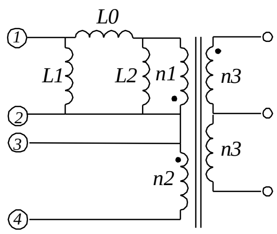

Fig.19 Electrical model of connecting dot-marked terminals

$$Lr = \frac{L1 \cdot L0}{L1 + L0} \qquad (9)$$

$$na = n2 - n1\frac{L1}{L1 + L0} \qquad (10)$$

$$Lm = L2 \cdot \frac{na^2}{n1^2} \cdot \frac{L1 + L0}{L1 + L2 + L0} \qquad (11)$$

Using the above-proposed model, the integrated magnetic component for this application can be designed. An integrated magnetic as shown in Fig.16 is designed as an example. To get the same value as discrete design (Lr=14uH, Lm=60uH and turn ratio=16:4), the design results of the integrated magnetic component are:

Nl=9, Np=13, Ns=4 and air gap is 0.56mm for all legs.

Fig.20 shows the simulated flux density on each leg. From simulation result it can be found that the flux density on center leg is greatly reduced. So with this integrated magnetic structure, the core loss could be greatly reduced. Also, with this structure, the air gap is the same for all legs, which is easier to manufacture and has less mechanical problem.

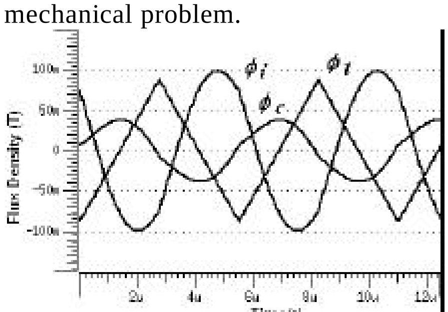

Fig. 20 Integrated Magnetic structure 3 and flux density in each leg

IV. Test Result

From above discussions, it can be found that integrated magnetic structure B provides better electrical performance due to the flux ripple cancellation effect in the center leg of the E core. It also has better manufacture capability and better mechanical stability due to factor that the three legs have the same length of air gap. To verify the design results, a prototype of integrated magnetic structure B is constructed and tested. The parameters are:

Lr=14uH, Lm=60uH and turn ratio=16:4.

Nl=9, Np=13, Ns=4 and air gap is 0.56mm for all legs.

The converter specs are:

Input voltage range: 300 to 400V

Output voltage: 48V

Output power: 1000W

Switching frequency range: 140kHz to 200kHz

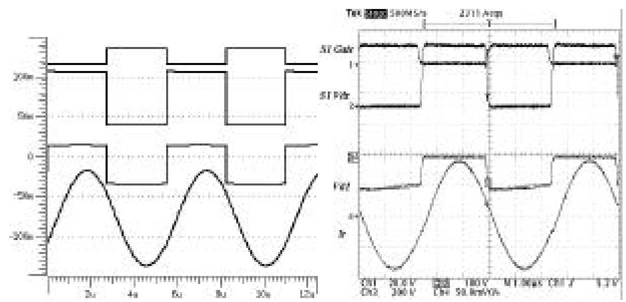

Fig. 21 Simulation waveform & test waveform for 400V input, fs=200kHz, full load

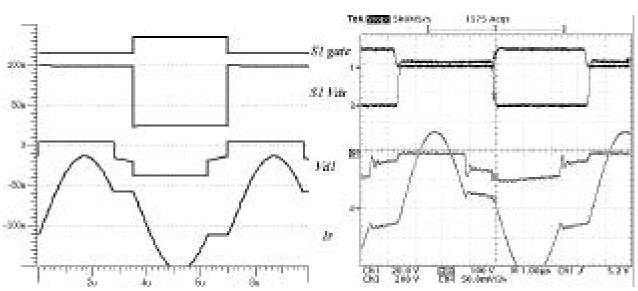

Fig. 22 Simulation waveform & test waveform for 300V input, fs=140kHz, full load

V. Conclusion

In this paper, integrated magnetic design for LLC resonant converter is discussed. Compared with discrete approach, integrated magnetic can reduce the components count and reduce the total core loss. Several integrated magnetic structures are also discussed in this paper. Integrated magnetic structure A is not preferred because the air gaps are only located on the outer legs, which will increase the complexity of manufacturing and decrease the mechanical stability. To investigate more structure, an electrical model for general structure is proposed based on the duality theory. Base on this model, structure B is proposed and analyzed. Compare with structure A, structure B provides better mechanical structure and better flux distribution. A prototype of structure B was constructed and tested. The experimental results verified the analysis and design results.

REFERENCES

[1] J.K. Watson, Applications of Magnetism, 1985

[2] Kats, A.; Ivensky, G.; Ben-Yaakov, "*Application of integrated magnetic in resonant converters*". APEC '97 Conference Proceedings 1997, Twelfth Annual, Volume: 2, 1997 Page(s): 925 -930 vol.2

[3] Chen, W.; Hua, G.; Sable, D.; Lee, F., "*Design of high efficiency, low profile, low voltage converter with integrated magnetics*" APEC '97 Conference Proceedings 1997., Twelfth Annual , Volume: 2 , 1997 Page(s): 911 -917 vol.2

[4] Peng Xu; Qiaoqiao Wu; Pit-Leong Wong; Lee, F.C., "*A novel integrated current doubler rectifier*" APEC 2000. Fifteenth Annual IEEE , Volume: 2 , 2000 Page(s): 735 -740 vol.2

[5] Bassett, I.A. "*Constant frequency ZVS converter with integrated magnetics*", APEC '92. Conference Proceedings 1992., Seventh Annual , 1992 Page(s): 709 -716